

An Innovative Hybrid Energy Storage System for Electric Vehicles

Sreelatha Jakkula¹, G.Praveen Kumar², Sameena Jilla³, Md.Khajafarid⁴, K.N.Bhanu Prakash⁵

^{1, 2, 3, 4} Assistant Professor, Department of Electrical and Electronics Engineering, Vaagdevi College of Engineering, Warangal, Telangana-506005, India.

⁵ Professor, Department of Electrical and Electronics Engineering, Vaagdevi College of Engineering, Warangal, Telangana-506005, India.

Abstract: This study introduces the design of a novel hybrid energy storage system tailored for electric vehicles, aiming to enhance long-distance endurance while minimizing cost. The research proposes an optimal control strategy for the hybrid energy storage system, leveraging the state of charge (SOC) of supercapacitors and employing a rule-based control method governed by the power dynamics of Li-ion batteries. Additionally, DC-DC converters utilized in electric vehicles are enhanced with a second-order Bessel low-pass filter through magnetic integration technology. This enhancement maximizes the power quality of the hybrid energy storage system while reducing the size of the battery. The efficacy of the proposed approach is validated through modeling and experimental analysis.

Keywords: Hybrid energy storage system, integrated magnetic structure, electric vehicles, DC-DC converter, power dynamic limitation.

Introduction

As society seeks solutions to combat the environmental impact of fossil fuels, continual advancements in new energy sources are being pursued [1-2]. Among these, lithium-ion (Li-ion) batteries have emerged as a prominent energy storage solution for modern electric vehicles due to their high energy density, facilitating long-distance endurance [3-4]. However, Li-ion batteries exhibit slower response times compared to supercapacitors [5]. To address this disparity and enhance the performance of electric vehicles, hybrid energy storage systems (HESS) combining both Li-ion batteries and supercapacitors are being adopted, aiming to achieve comparable long-distance endurance, energy, and rapid acceleration to conventional fuel-powered vehicles [5]. Optimizing energy storage devices is paramount for advancing electric vehicle technology, necessitating the expansion of battery capacity while simultaneously reducing size and weight to improve charging rates [6-8].

The rapid evolution of DC-DC converters, pivotal components in hybrid energy storage systems, has been witnessed over recent years. Various innovations have been proposed to enhance the capabilities of DC-DC converters. For instance, a novel zero Voltage Switch (ZVS) bidirectional DC-DC converter has been introduced [9], although its complex management and higher cost render it unsuitable for widespread adoption in electric vehicles, despite its potential to enhance conversion efficiency. Alternatively, an isolated, bi-directional DC-DC converter [10] with a complex topology has demonstrated proficiency in handling large power transmissions. Furthermore, the pioneering work of S. Cuk introduced a novel zero-ripple switching DC-to-DC converter integrated with magnetic technologies [11-12], showcasing significant success in practical applications. Another innovation, the isolated interleaved DC/DC converter [13], introduced the concept of three-winding coupled inductors, albeit more suited for power transmission purposes.

Effective energy management strategies are crucial for maximizing the performance of hybrid energy storage systems. A diverse array of energy management techniques, including neural networks, fuzzy logic, state machine control, frequency decoupling, optimal strategies (both online and offline), dynamic programming (DP), and battery power limiting, have been extensively explored in the literature [14–17]. The primary objective of these control strategies is to minimize a cost function while ensuring continuous power supply. These strategies can be categorized into offline global optimization and online local optimization methods. Offline global optimization requires obtaining the optimal power allocation among various energy sources, while online local optimization necessitates accurate prediction of driving conditions [18–20].

This paper proposes the utilization of an innovative integrated magnetic structure for DC-DC converters in hybrid energy storage systems for electric vehicles. The proposed DC-DC converter facilitates control over Li-ion batteries and supercapacitors, incorporating specific topology and operating modes. Furthermore, an optimization control algorithm based on the state of charge (SOC) of the supercapacitor is introduced, employing a Li-ion battery power dynamic limitation rule-based control approach for energy management. To optimize control parameters and enhance the longevity and size reduction of the hybrid energy storage system, a hybrid optimization method combining particle swarm optimization and the Nelder-Mead simplex approach is employed. Ultimately, the performance of the hybrid energy storage system is validated through modeling and experimental research.

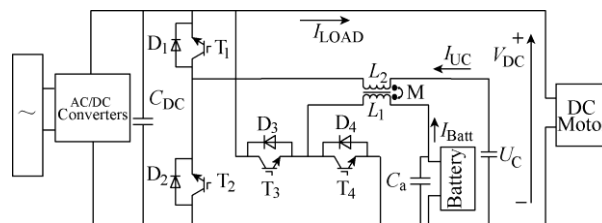


Fig. 1: Topology of the hybrid energy storage system

The proposed hybrid energy storage system comprises a Li-ion battery, supercapacitors, and a DC/DC converter. The DC/DC converter consists of four IGBT switches (T1–T4) and corresponding diodes (D1–D4), along with an integrated magnetic structure consisting of self-inductance (L1–L2) and mutual inductance (M) sharing a core inductor. The battery pack powers the smooth DC motor, while the supercapacitor manages instantaneous peak power supply. Electric vehicle power management systems regulate electrical energy flow based on load requirements.

The converter operates in five primary modes, as shown in Table 1, depending on the additional battery pack modification, with each mode facilitating specific energy flows within the hybrid energy storage system.

Design of the DC/DC converter with integrated magnetic structure

The fundamental components for energy conversion, filtration, electrical isolation, and energy storage rely on magnetic devices such as inductors. The size and weight of the converter are significantly influenced by the size of the magnetic elements. To achieve integration of magnetic elements, an E-type magnetic core is utilized in this study, incorporating coupling inductances (L1 and L2) as illustrated in Fig. 2. Here, L2 functions as the output filter inductor, L1 as the external inductance, and Ca as additional capacitance.

In steady state conditions, the voltage across Ca equals the output voltage of L2 and L1 without considering the capacitor voltage ripple. The DC/DC converter depicted in Fig. 1 consists of four IGBT

Volume 10 Issue 5 - May 2022 - Pages 1-1

switches (T1–T4) and four diodes (D1–D4). Two operational modes exist for a boost converter—L1, T4, D4, or L2, T2, D1—and three operational modes for a buck converter—L1, T3, D4, or L2, T1, D2.

Table 1: Operation Mode of Hybrid Energy Storage System

Working Mode	Power Source	Power Flow	Operation Mode
Parking Charging Mode	AC Power	Battery and Supercapacitor	Buck
Constant Speed Mode	Battery	DC Motor Voltage	Boost
		Cdc is the capacitor DC motor, D is the duty cycle. In the frequency range, the relationship	
Acceleration Mode	Supercapacitor	DC Motor	Boost
Braking Mode	Braking Energy	Battery and Supercapacitor	Buck
Super-capacitor Charging Mode	Battery		

Table 2: Comparison of Two Structures of DC/DC Converter

Feature	Discrete Inductors Structure (cm ²)	Integrated Magnetic Structure (cm ²)	Effect (%)
Surface Area	79.15	60	-24.20

Table 2 compares two DC/DC converter constructions, highlighting the compactness and reduced weight achieved with the DC/DC converter integrated with a magnetic structure. Utilizing such a converter can decrease the overall size and weight of the energy storage system in an electric vehicle, while also reducing output current ripple. Section 4 presents simulation and experimental results validating the performance of the integrated magnetic structure.

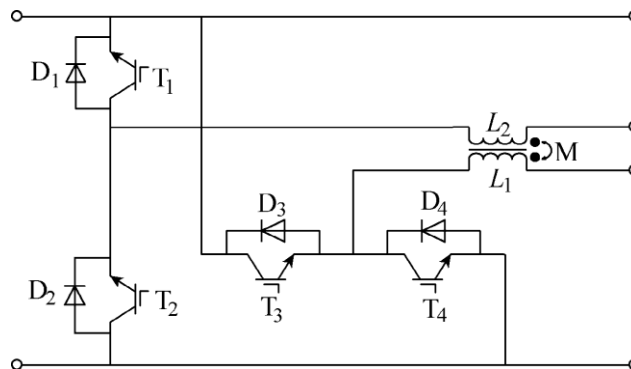


Figure 2 illustrates the topology of the DC/DC converter featuring an integrated magnetic structure.

The control strategy of the hybrid energy storage system involves the implementation of cascade voltage and current controllers to ensure a stable load voltage. Super-capacitors, known for their quick response, are utilized to recycle braking energy during voltage spikes on the DC side. The control block diagram of the super capacitor controller is depicted in Figure 3, where f_s represents the switching frequency, G_1 and G_2 denote the switching signals of T_1 and T_2 , and V_{dc} and V_{dc-sen} represent the actual voltage and rated voltage of the DC motor, respectively. Additionally, i_{UC}^* and $i_{(UC-sen)}^*$ denote the real current and rated current per unit of the super-capacitor.

The Li-ion battery, on the other hand, supplies steady DC motor current through battery pack control. To reduce output current ripples and mitigate abrupt fluctuations, a second-order Bessel low-pass filter with a cut-off frequency of 50Hz is employed. Assuming the converter is lossless, the DC motor current equals the battery current, as expressed in Equation (3).

The reference current of the battery pack is determined based on the state of charge (SOC) of the super-capacitor. If the SOC of the super-capacitor falls below the lower limitation $Q_{sc_char_low}$, the limitation of Li-ion power is adjusted to $P_{char_low_limit}$, as per Equation (4). The dynamic limitation of the Li-ion battery is governed by Equations (5) and (6).

During discharging of the hybrid energy storage system, if the SOC of the super-capacitor surpasses the upper limitation $Q_{sc_disch_high}$, the limitation of Li-ion power is increased to $P_{disch_high_limit}$. Conversely, if the SOC of the super-capacitor drops below the lower limitation $Q_{sc_disch_low}$, the limitation of Li-ion power is reduced to $P_{disch_low_limit}$, as described in Equations (8) and (9).

To prevent frequent switches between charge and discharge modes and alleviate strain on the Li-ion batteries, a rule-based control system for Li-ion battery power dynamic limitation, based on the super capacitor's state of charge, is implemented. The operating modes are summarized as follows:

Mode 1: Charging mode - Adjust Li-ion power limitation based on super-capacitor SOC. Mode 2: Discharging mode - Modify Li-ion power limitation based on super-capacitor SOC. Figure 4 illustrates the block diagram of the Li-ion battery pack control.

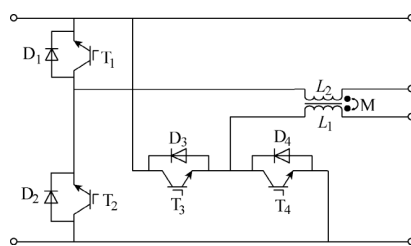


Fig. 2: Topology of DC/DC Converter with Integrated Magnetic Structure

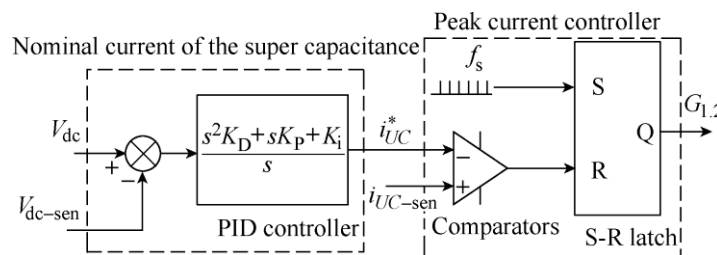


Fig. 3: Block Diagram of the Super Capacitor Voltage and Current Controller

Volume 10 Issue 5 - May 2022 - Pages 1-1

The selection of a cascade voltage and current controller ensures a steady load voltage supply in the hybrid energy storage system. Super-capacitors exhibit rapid response times and facilitate the recuperation of braking energy during instances of significant increases in the DC side voltage while braking. The control block diagram of the super capacitor controller is depicted in Fig. 3, where f_s represents the switching frequency, G_1 and G_2 denote the switching signals of T_1 and T_2 , and V_{dc} and V_{dc-sen} correspond to the actual voltage and rated voltage of the DC motor, respectively. Additionally, i_{UC}^* and $i_{(UC-sen)}^*$ represent the real current and rated current per unit of the super-capacitor.

Table 1: Operation Modes of the Hybrid Energy Storage System

Operating Mode	Power Source	Power Flow	Operation Mode
Constant Speed Mode	AC Power	Battery and Super Capacitor	Buck
	Battery	DC	Boost

$$I(L2(S))/DS=(Vdc \times Rload \times CDC \times S^2 + L2 \times S + Rload \times (1-D)^2)(Vdc \times Rload \times CDC \times S + 2VDC)$$

Table 2: Comparison of Two Structures of DC/DC Converter

Feature	Acceleration Mode	Braking Mode
	Supercapacitor	DC Motor
Discrete Inductor Structure/cm ²	79.15	60
Integrated Magnetic Structure/cm	104.19	79.60
Braking Energy	-24.20	-23.60
Battery and Super Capacitor	Super Capacitors and DC Motors	Battery
Surface Area		
Super-Capacitor Charging Mode	Battery	Super Capacitors and DC Motors
Core Volume		
Core Weight/kg	0.31	0.23
Wire Weight/kg	0.21	0.21

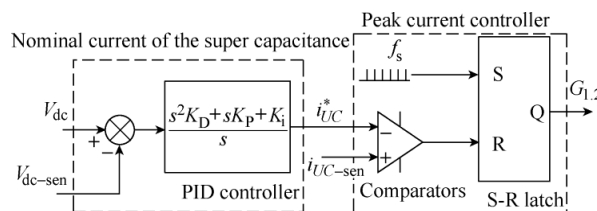


Fig.3 Block diagram of the super-capacitor voltage and current controller

The DC motor current can be supplied steadily by the battery pack controller. The 50Hz Bessel low-pass filter's second-order cutoff frequency has been used to lessen output current ripples and prevent abrupt, significant fluctuations.

Assuming the converter is lossless, the DC motor current is equal to the battery current, which can be expressed as:

$$V_{load} \times I_{load} = V_{batt} \times I_{batt}; I_{batt} = V_{batt} / V_{load} \times I_{load} \quad (3)$$

The reference current of the battery pack is expressed as:

$$I^* = V_{load} \times I_{load} \times G(s) \quad (4)$$

Reduced to char_low_limit $P_{char_low_limit}$, the dynamic limitation of the Li-ion battery can be written as:

$$batt(6) / LP_{batt}(6)$$

Where V_{load} / I_{load} and V_{batt} / I_{batt} stand for the voltage and current of the DC motor; V_{batt} / I_{batt} and V_{load} / I_{load} are the voltage and current of the Li-ion battery.

$$GLP(s) = sn + a(2)sn - 1 + \dots + a(n + 1) \left(\frac{s}{\omega_0} \right) \quad (5)$$

Mode 2: When the HESS is discharging, if the SOC of the super-capacitor exceeds the upper limitation sc_disch_high $Q_{sc_disch_high}$, the limitation of Li-ion power is increased to $disch_high_limit$ $P_{disch_high_limit}$; if the SOC of the super-capacitor is lower than the lower limitation sc_disch_low $Q_{sc_disch_low}$, the limitation of Li-ion power is reduced to $disch_low_limit$ $P_{disch_low_limit}$. The dynamic limitation of the Li-ion battery can be written as:

$$P_{bat_disch_limit} = P_{disch_high_limit} \quad (8)$$

$$bP_{bat_disch_limit} = P_{disch_high_limit} \quad (9)$$

Furthermore, to prevent frequent Li-ion battery switches (charge and discharge) and lessen the strain on the Li-ion batteries, a rule-based control system for Li-ion battery power dynamic limitation based on the supercapacitor's state of charge has been implemented.

The operating modes are as follows:

Mode 1: When the HESS is charging, if the SOC of the super-capacitor exceeds the upper limitation $Q_{sc_char_high}$, the limitation of Li-ion power is increased to $char_high_limit$.

5.2 Simulation and Experiment of Proposed HESS Applied to Electric Vehicles

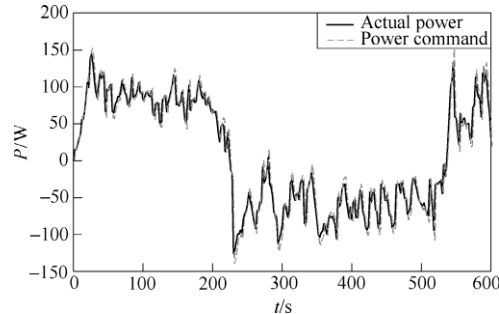
5.2.1 Simulation

In order to assess the dynamic performance of the system, a simulation model of the proposed Hybrid Energy Storage System (HESS) applied to a typical car driving cycle was developed using Matlab/Simulink. The parameters of the simulation system are presented in Table 5.

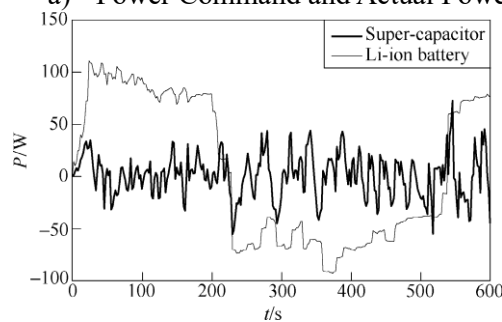
Using Matlab/Simulink, simulations are conducted to emulate various driving scenarios including acceleration, constant speed, braking, and parking charging modes. Throughout these simulations,

Volume 10 Issue 5 - May 2022 - Pages 1-1

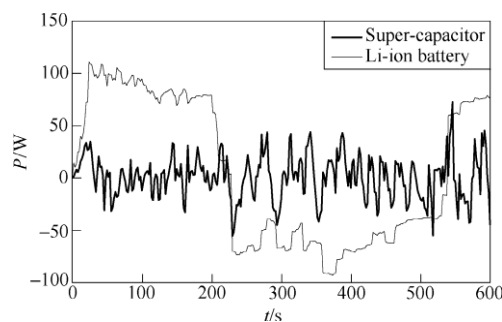
particular attention is paid to observing the stability of parameters such as load side voltage, battery performance, and supercapacitor current ripple.



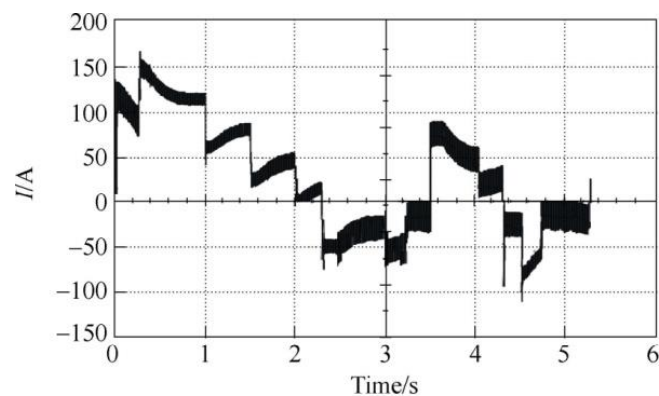
a) Power Command and Actual Power



(b) Power of the Supercapacitor and Li-ion Battery



(a) Battery current



(b) Super-capacitor current

5.2.2 Experiment

In this section, an experiment is conducted to observe variations in battery and supercapacitor currents in response to step changes in the load. A small-scale experiment was constructed, utilizing a boostcap PC2500 supercapacitor to fulfill the requirements within a laboratory setting. The switches employed in the experiment are HGTG30N60A4D IGBTs, while the voltage and current sensors utilized are LV 20-P and LA100-P, respectively. The feedback and control system chosen is the TMS320F2812 DSP. Inductors L1, L2, and M have respective values of 2 mH, 50 μ H, and 50 μ H. Actual values for these devices are listed in Table 6.

The exceptional response of the proposed HESS to braking and accelerating conditions of electric vehicles is demonstrated in Figure 9. In energy storage systems utilizing supercapacitors, when the load increases at $t=3$, the battery current smoothens out and follows a slow, controlled ramp; simultaneously, the supercapacitor discharges at a high frequency rate, stabilizing the DC voltage at 20V with less than 5% overall volatility. When the load decreases at $t=7$, the supercapacitor recovers the braking energy, evident by the negative supercapacitor current. In contrast, in an energy storage system relying solely on a battery pack without supercapacitors, the battery bears the brunt of load adjustments, leading to significant current fluctuations and ripple, consequently shortening the battery's lifespan. Compared with the proposed HESS, such a system is deemed unsuitable for electric vehicles.

6 Conclusions

This study introduces the design of a novel hybrid energy storage system for electric vehicles, based on a new bi-directional DC/DC converter and a Li-ion battery power dynamic limitation rule-based HESS energy management.

Table 6: Experimental Equipment and Circuit Parameters

Experimental Data	
DC Side Voltage (V)	$V_{dc}=20$
Battery Voltage (V)	$V_{batt}=12$
Initial Charge State	80% Lead-acid battery
Supercapacitor	Maxwell Boostcap PC2500 series connection, 450450F, initial state of charge 12V
Switching Frequency (kHz)	$f_s=20$
Sampling Time (μs)	$T_{st}=20$
DSP Model	TI-TMS320F2812
Inductors $L1, L2$ (μH)	1.938mH, 54.5687
Inductor M (μH)	52.786652.7866
Switch Model	HGTG30N60A4D IGBT

Volume 10 Issue 5 - May 2022 - Pages 1-1

Voltage Sensor	LV20-P
Current Sensor	LA100-P

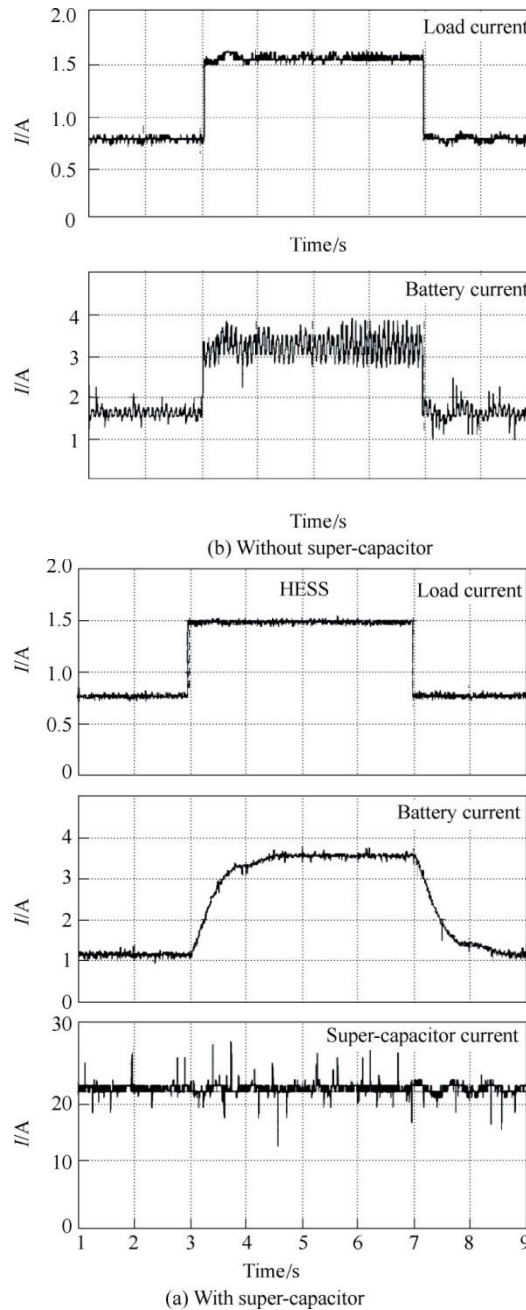


Figure 9: Experiment Results of the Proposed HESS Applied on Electric Vehicles

Comparison with a conventional hybrid energy storage system highlights the advantages of the proposed system, including lower volume and weight, extended battery life, and reduced output current ripple.



REFERENCES

1. Zhikang Shuai, Chao Shen, Xin Yin, Xuan Liu, John Shen, "Fault analysis of inverter-interfaced distributed generators with different control schemes," IEEE Transactions on Power Delivery, DOI: 10.1109/TPWRD.2017.2717388.
2. Zhikang Shuai, Yingyun Sun, Z. John Shen, Wei Tian, Chunming Tu, Yan Li, Xin Yin, "Microgrid stability: classification and a review," Renewable and Sustainable Energy Reviews, vol. 58, pp. 167-179, Feb. 2016.
3. N.R. Tummuru, M.K. Mishra, and S. Srinivas, "Dynamic energy management of renewable grid integrated hybrid energy storage system," IEEE Trans. Ind. Electron., vol. 62, no. 12, pp. 7728-7737, Dec. 2015.
4. T. Mesbahi, N. Rizoug, F. Khenfri, P. Bartholomeus, and P. Le Moigne, "Dynamical modelling and emulation of Li-ion batteries-supercapacitors hybrid power supply for electric vehicle applications," IET Electr. Syst. Transp., vol. 7, no. 2, pp. 161-169, Nov. 2016.
5. A. Santucci, A. Sornioti, and C. Lekakou, "Power split strategies for hybrid energy storage systems for vehicular applications," J. Power Sources, vol. 258, no. 14, pp. 395-407, 2014.
6. J. Shen, S. Dusmez, and A. Khaligh, "Optimization of sizing and battery cycle life in battery/ultracapacitor hybrid energy storage systems for electric vehicle applications," IEEE Trans. Ind. Informat., vol. 10, no. 4, pp. 2112-2121, Nov. 2014.
7. M. Ecker, J.B. Gerschler, J. Vogel, S. Käbitz, and F. Hust, "Development of a lifetime prediction model for lithium-ion batteries based on extended accelerated aging test data," J. Power Sources, vol. 215, no. 5, pp. 248-257, Oct. 2012.
8. R. Sadoun, N. Rizoug, P. Bartholomeus, B. Barbedette, and P. Le Moigne, "Optimal sizing of hybrid supply for electric vehicle using Li-ion battery and supercapacitor," In Proc. IEEE Veh. Power Propulsion Conf., pp. 1-8, 2011.
9. D. Liu, and H. Li, "AZVS bi-directional DC-DC converter for multiple energy storage elements," Transactions on Power Electronics, vol. 21, no. 5, pp. 1513-1517, 2006.
10. N.M.L. Tan, T. Abe, and H. Akagi, "Design and performance of a bidirectional isolated DC-DC converter for a battery energy storage system," IEEE Transactions on Power Electronics, vol. 27, no. 3, pp. 1237-1248, 2012.
11. S. Cuk, R.D. Middlebrook, "A new optimum topology switching DC-to-DC converter," In: Proceedings of 8th IEEE Power Electronics Specialists Conference, pp. 160-179, 1977.
12. S. Cuk, "A new zero-ripple switching DC-to-DC converter and integrated magnetics," IEEE Transactions on Magnetics, vol. 19, no. 2, pp. 57-75, 1983.
13. Wuhua Li, Xiangning He, Jianyong Wu, "Isolated interleaved DC/DC converters with winding-cross-coupled inductors," Transactions of China Electrotechnical Society, vol. 24, no. 9, pp. 99-106, 2009.
14. M. E. Choi, S. W. Kim, and S. W. Seo, "Energy management optimization in a battery/supercapacitor Hybrid energy storage system," IEEE Trans. Smart Grid, vol. 3, no. 1, pp. 463-472, Mar. 2012.



Volume 10 Issue 5 - May 2022 - Pages 1-1

15. Z. Yu, D. Zinger, and A. Bose, "An innovative optimal power allocation strategy for fuel cell, battery and supercapacitor hybrid electric vehicle," J. Power Sources, vol. 196, no. 4, pp. 2351-2359, Feb. 2011.
16. Zhikang Shuai, Yang Hu, Yelun Peng, Chunming Tu, Z. John Shen, "Dynamic stability analysis of synchronverter-dominated microgrid based on bifurcation theory," IEEE Transactions on Industrial Electronics, vol. 64, no. 9, pp. 7467-7477, Sep. 2017.
17. Q. Li, W. Chen, Y. Li, S. Liu, and J. Huang, "Energy management strategy for fuel cell/battery/ultracapacitor hybrid vehicle based on fuzzy logic," Int. J. Electr. Power Energy Syst., vol. 43, no. 1, pp. 514-525, Dec. 2012.
18. Zhikang Shuai, Wen Huang, Chao Shen, Jun Ge, and Z. John Shen, "Characteristics and restraining method of fast transient inrush fault currents in synchronverters," IEEE Transactions on Industrial Electronics, vol. 64, no. 9, pp. 7487-7497, Sep. 2017.
19. A. Castaings, W. Lhomme, R. Trigui, and A. Bouscayrol, "Comparison of energy management strategies of a battery/supercapacitors system for electric vehicle under real-time constraints," Appl. Energy, vol. 163, pp. 190-200, 2016.
20. S.K. Kollimalla, M.K. Mishra, and N.L. Narasamma, "Design and analysis of novel control strategy for battery and supercapacitor storage system," IEEE Trans. Sustain. Energy, vol. 5, no. 4, pp. 1137-1144, Oct. 2014.